Article

Reaction Kinetic Study of Solketal Production from Glycerol Ketalization with Acetone

Vinicius Rossa, Yolanda da S. P. Pessanha, Gisel Ch Díaz, Leôncio
Diógenes Tavares Câmara, Sibele B C Pergher, and Donato A. G. Aranda

Just Accepted

Reaction Kinetic Study of Solketal Production from Glycerol Ketalization with Acetone

Vinicius Rossa[¥]*, Yolanda da S. P. Pessanha[¥], Gisel Ch. Díaz[¥], Leôncio Diógenes Tavares Câmara[†], Sibele B. C. Pergher [‡] and Donato A. G. Aranda[¥].

[¥] Laboratório GreenTec, UFRJ, Av. Horácio Macedo, 2030, Rio de Janeiro – RJ. CEP: 21941-909, Brasil.

[†] Departamento de Engenharia Mecânica e Energia (DEMEC), Instituto Politécnico da Universidade do Estado do Rio de Janeiro (IPRJ-UERJ), Nova Friburgo-RJ, CEP 28625-570, Brasil.

[‡] Laboratório de Peneiras Moleculares, UFRN, Av. Senador Salgado Filho, 3000. Natal – RN. CEP 59078-970, Brasil.

KEYWORDS: Glycerochemistry, Solketal, H-BEA, Kinetics Study.

ABSTRACT: The best conditions for the kinetic study of the ketalization reaction of glycerol with acetone for the production of Solketal using zeolite H-BEA (SAR 19) as a catalyst were found through a fractional experimental design. To simplify the heterogeneous kinetics, by means of a smaller number of kinetic parameters to encompass all the kinetic terms towards the products and reagents, a reversible kinetic model was used. From the comparison between the

experimental and calculated conversions, it was possible to analyse the accuracy of the estimations, providing a good way to apply statistical treatments to improve the calculated kinetic properties. Thereby, it is possible to calculate the equilibrium constants for a range of reactions performed across different temperatures (40-80°C) as well as the forward reaction activation energy (44.77 kJ mol^{-1}) and the reverse reaction activation energy (41.40 kJ mol^{-1}). Moreover, 70-76% glycerol conversion was obtained using the same catalyst for five reactions, without wash or performing any other pre-treatments in the catalyst between reactions. The Solketal product has been studied as a green industrial solvent additive in gasoline and biofuels.

1 – INTRODUCTION

The latest version of nomenclature of organic chemistry has been recently published by the International Union of Pure and Applied Chemistry (IUPAC, 2013). It includes the new terminology for glycerol, named propane-1,2,3-triol, which refers to an alcohol function in its organic chain that includes three hydroxyl groups. However, this denomination is only applicable to the pure compound (100%) that is produced by fine chemical industries. The molecular formula of glycerol is $C_3H_8O_3$, and it was discovered in 1779 by a Swedish scientist called Carl Wilhelm Scheel while conducting experiments on heating lead oxide and an olive oil mixture. The term glycerin refers to a commercial reactant containing an average of 95% of glycerol. Furthermore, there are several types of commercial glycerin with various characteristics such as variations in colour, odour, concentration, and impurities[1].

Through the global success of biodiesel industry, glycerin production has shown a steep rate of growth. Approximately 100 mL of crude glycerin can be generated for each litre of

biodiesel produced, i.e., 10% [2, 3]. Although there is a range of manufactured products using glycerin in its formulation, the used amount is not sufficient to employ the all glicerin produced by the biodiesel industry. Therefore, new technological improvements in converting the excess glycerin into value-added products must be made [1, 4].

There are some reaction types in which glycerol may be transformed into other chemicals, including acetalization [1, 5-8], ketalization [1, 9-18], carbonation [1, 19-28], dehydration [1, 20, 29] etherification [1, 20, 30-32], esterification [1, 33-36], hydrogenolysis [1, 37- 42], and oxidation [1, 20, 43, 44], among others. The ketal is known industrially as Solketal, isopropylidene glycerol or, according to IUPAC, as (2,2-dimethyl-1,3-dioxolan-4-yl) methanol. It is produced via the ketalization reaction of glycerol with acetone. Unlike acetalization, in which glycerol is reacted with an aldehyde, in the ketalization reaction, glycerol is reacted with an acetone. In either case, the reactions are facilitated via a homogeneous (sulfuric acid, hydrochloric acid, phosphorus pentoxide, and p-toluenesulfonic acid) or heterogeneous acid catalyst (zeolites, clays, and Amberlyst resins) [9]. A range of glycerol ketals and acetals can be produced with a variety of ketones and aldehydes, respectively [10]. These compounds have significant potential when applied as fuel additives and biofuels. Solketal may be a suitable additive for the formation of gasoline, diesel and biodiesel. It may be used to improve fuel properties, decrease viscosity and help obtain standard requirements of biodiesel flash point and oxidation stability [9,10].

Moreover, glycerol ketals are used as solvents, plasticizers, surfactants, disinfectants, and flavourings, among other applications. These compounds can be used both in the pharmaceutical industry and in the food industry [1, 9, 10]. Ketalization generates glycerol branched oxygenates (**Scheme 1**). However, when ketalization is carried out with acetone, there is greater selectivity (≈98.0%) for the solketal molecule (2,2-dimethyl-[1,3]dioxolan-4-yl)-methanol, a five membered

ring. Furthermore, this reaction is less selective ($\approx$2.0%) towards producing 2,2-dimethyl-[1,3]dioxan-5-ol, a six membered ring [9].
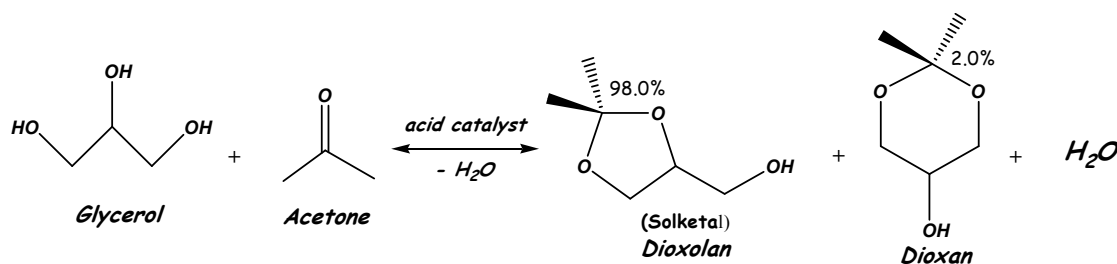
Scheme 1. Ketalization reaction between glycerol and acetone (Adapted from [10]).

In fact, solketal is a molecule in which its hydroxyls are protected, suggesting that the compound is a preserved type of glycerol. The interaction between 1,3 carbons that occurs among the chain carbons provided by acetone as well as by the β-carbon hydrogen may be the main factor in explaining the low selectivity towards the formation of 2,2-dimethyl-[1,3]dioxan-5-ol. Thus, the β-carbon hydrogen interaction is more intense than that with 1,1-dimethyl cyclohexane due to the shorter carbon-oxygen bond length of 1.43 Å [11]. Industrially, the solketal reaction is catalysed by p-toluenesulfonic acid (PTSA) Brönsted acid that is used in homogeneous catalysis for 12 h at 100°C [13].

Homogeneous catalysts, in this case, Brönsted acids such as hydrochloride acid, sulfuric acid, p-toluenesulfonic acid and others, have some drawbacks that reduce their applicability. In particular, these catalysts can cause corrosion in the reactors, they cannot be reused, and they are difficult to separate from products and reactants after the chemical reaction process. The Menezes group (2013) has proposed the use of homogeneous catalysts of the Lewis acid type [$SnCl_2$, SnF_2, $Sn(OAc)_2$] that are easily recovered. Based on their results, $SnCl_2$ is the most

effective catalyst, with a 77% conversion and 98% selectivity for the synthesis of solketal at 60°C. In addition to being easily recoverable during distillation of the reaction mixture, the catalyst may be reused up to 6 times [14]. However, in industrial processes, the presence of chlorides (Cl^- from the $SnCl_2$) in the reaction medium is undesirable because they cause corrosion in the reactors and in other pipes. The major trend of the twenty-first century is to replace most of the chemical processes that involve the use of homogeneous catalysts with heterogeneous catalysts [45, 46, 47]. There are many advantages for using heterogeneous catalysts, such as less effort in separating the catalysts, the possibility of using higher temperature ranges, their reuse, recycling of the catalyst, an average selectivity and a lower price. However, they present some difficulties, such as in maintaining surface stability, keeping desirable surface properties and avoiding char formation [48, 49].

The Amberlyst-15 resin, zeolite beta [16] and the heteropolyacid PW-S [15] are the catalysts that showed the most promising activity for the ketalization reaction of glycerol with acetone, with conversions of 95, 90, 94% and selectivities of 95, 90 and 97%, respectively. Related studies and kinetic ketalization modelling reactions between glycerol with acetone are present in the literature [50, 51].

This work presents a study of the kinetics of glycerol ketalization with acetone and H-BEA zeolite catalyst for the Solketal production. The use of H-BEA zeolites in catalysis is attributed to their high thermal, hydrothermal and mechanical stability. Their stability improves with as the Si/Al ratio of the structure increase. The H-BEA catalyst easily regenerated by the burning of coke between 500 and 700 °C.

A reversible kinetic model was assumed in the determination of the kinetic parameters for the reaction. From the experimental equilibrium data, it was possible to determine the accuracy

of the estimations and determine the kinetic parameters of the studied reactions at different temperatures[52, 53]. It was also possible to calculate the activation energy, Ea, for this process, using the Arrhenius equation. Moreover, the performance of catalysts upon reuse was investigated.

2 – EXPERIMENTAL

2.1 – Reactants

Glycerol (99.5% A.S.) and acetone (99.5% A.S.) used in the present work were supplied by the Brazilian chemical plant PROQUIMIOS.

2.2 – Catalyst

BEA zeolite (SAR 19) from Zeolyst International has been used as a catalyst in this work. In fact, the acquired zeolite ammonium type (BEA- NH_4^+) was calcined in a muffle oven at 500°C/4 h with a ramp of 10°C/min. Then, the solid was stored in a warm oven at 100°C to prevent contact with water while it was waiting to be used in reactions. After these steps, the H-BEA catalyst type of zeolite was ready to catalyse the ketalization reaction. The main characteristics after the calcining stage included the following: a BET area of 536 m² g^{-1} according to the Brunauer-Emmett-Teller (BET) method, a total volume of 0.57 cm³ g^{-1} and a mean pore diameter of 13.7 nm determined via the Barret-Joyner-Halenda (BJH) method. The characteristics of the Brönsted acid sites (BS) and Lewis acid sites (LS) after different temperature treatments of zeolites (µmol pyridine/g of material) were as follows: T150°C (BS60.42 and LS33.65), T250°C (BS39.24 and LS58.13), and T350°C (BS24.17 and LS45.91).

A total of 9.41 $\times$ 10^{-5} mols of acid sites/g cat was calculated using the results of FTIR-Py analysis at 150 °C.

The spectra were recorded, and then pyridine was added. After equilibration, the samples were outgassed for 1 h at increasing temperature (150/250/350°C). After each desorption step, the spectrum was recorded at room temperature, the background was subtracted in the pyridine case, and absorption coefficients calculated by Emeis (1993) were used [61].

2.3 – Investigation of the Best Conditions for the Kinetic Study

A fractional factorial design type (2^{4-1}) was chosen to investigate the best conditions for the kinetic study [54]. The process was conducted in a PARR 4842 model autoclave reactor by the Parr Instrument Company, with a volume of 300 mL. The system consists of a thermocouple, an external ceramic fibre heater, and temperature and stirring controllers. The reactor was fed with 40 g of glycerol (0.43 mols). Then, the following variables were changed: stirring (S) (400; 550; 700 rpm), temperature (T) (40; 50; 60°C), catalyst amount (C) (1, 3, or 5%, relative to the mass of glycerol in this process), and finally, the molar ratio of glycerol:acetone (G:A), called RM (1:2; 1:3; 1:4). Additionally, the reaction time was set to exactly 1h. Fractional Experimental Planning (2^{4-1}) consisted of 8 experiments with the addition of three central points (for experimental error calculation). Hence, a total of 11 experiments were carried out to determine optimum Conversion (X_A) and Selectivity (S_S).

2.4 – Kinetic Studies

Kinetic studies were conducted in the same reactor system equipment that was used for the Fractional Experimental Planning, which was mentioned earlier. Thus, the reaction samples were collected between 5 and 180 min. Upon the completion of gas chromatographic analyses, it was possible to plot a kinetic curve showing a relationship between H-BEA catalyst capacity and temperature (40, 50, 60, 70 and 80°C).

2.5 – Determination of kinetic parameters

The elementary reaction is shown in **Eq. 1**, as follows:

$$aA + bB \underset{k_{-1}}{\overset{k_1}{\rightleftharpoons}} cC + dD \qquad \text{(Eq. 1)}$$
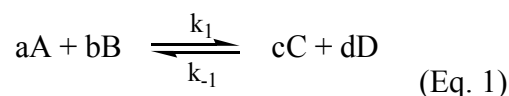
In this case, the letters A and B represent reactants, i.e., glycerol and acetone, while C and D represent solketal products and water, respectively. Additionally, (a, b, c, and d) correspond to species coefficients in those reactions. For the determination of kinetic parameters, a reversible kinetic model was used, according to **Eq. 2**.

$$\frac{dC_{Solketal}}{dt} = k_1.C_A C_B - k_{-1}.C_C.C_D \qquad \text{(Eq. 2)}$$

where, C is the molar concentration of the species involved (C_A, C_B, C_C, and C_D) in the reaction, k_1 is the formation constant of products, and k_{-1} is the constant of the reverse reaction. The correlation of experimental data for the calculation of k_1 and k_{-1} was carried out using a simulator for the determination of kinetic parameters.

The reaction of ketalization was modelled via a reversible kinetic model (Eq. 2) with the kinetic constants k_1 and k_{-1} related to the forward and reverse reaction, respectively. To calculate the kinetic constants k_1 and k_{-1}, the correlation with the experimental data was performed utilizing the inverse stochastic routine R2W (Random Restricted Window).

Accounting for the stoichiometric coefficients, we consider that the reaction order is equal to 1 for each component [53]. The data required as input for this simulation include the reactor volume (mL), mass (g) of glycerol, molecular weight (g mol^{-1}) of glycerol, mass (g) of acetone, molecular weight (g mol^{-1}) of the acetone conversion, and the experimental results (X_A%) at each time (min) of the reaction. The R2W is a simple method of searching random estimations in the domain of the parameters.

Using the reversible model, we can simplify the complex kinetics of heterogeneous reaction via a smaller number of parameters. Thus, the parameters k_1 and k_{-1} encompass all kinetic terms of the products and reagents, respectively.

A better solution is obtained via the function of squared residue, Q, which in turn is obtained by comparing the glycerol conversions observed experimentally ($X_{A\ EXP}$) and theoretically calculated ($X_{A\ CAL}$), **Eq. 3**. In other words, by minimizing the sum of the squares of the residuals, we can determine how much the simulated curve approaches reality. A statistically accepted Q value, in this case, would be $0 \geq Q < 300$.

$$Q = \sum_{i=1}^{n} \left(X_{A_{CAL}} - X_{A_{EXP}} \right)^2 \quad \text{(Eq. 3)}$$

Initially, in this inverse routine, there is a random estimation of parameters. After the determination of the best solution, there is a new restricted search near the best solution encountered in a previous step. The good fit of the model together with the experimental data shows the potential of the approach in the representation of the reaction system.

The k_1 and k_{-1} values were used to determine the equilibrium constant (**Eq. 4**). Then, the theoretical conversion values were calculated (**Eq. 5**).

$$K_{eq} = \frac{k_1}{k_{-1}} \quad \text{(Eq. 4)}$$

$$K_{eq} = \frac{C_C.C_D}{C_A.C_B} \quad \text{(Eq. 5)}$$

In **Eq. 5,** considering the reaction stoichiometry, the equilibrium constant is related to the concentration of the species. The concentration of compounds may be converted through a factor that is determined via the equilibrium constant value [53]. It was possible to calculate the equilibrium glycerol conversion $X_{A\,eq}$, assuming $C_{A0} = C_{B0}$ in **Eq. 6,** as follows:

$$K_{eq} = \frac{(C_C)_{eq}.(C_D)_{eq}}{(C_A)_{eq}.(C_B)_{eq}} = \frac{(C_{A0}.X_{Aeq})^2}{C_{A0}^2.(1-X_{Aeq})^2} = \frac{X_{Aeq}^2}{(1-X_{Aeq})^2} \Rightarrow X_{Aeq} = \frac{\sqrt{K_{eq}}}{(1+K_{eq})} \quad \text{(Eq. 6)}$$

Then, when $C_{A0} > C_{B0}$, **Eq. 7** can be generated as follows:

$$K_{eq} = \frac{(C_C)_{eq}.(C_D)_{eq}}{(C_A)_{eq}.(C_B)_{eq}} = \frac{(C_{A0}.X_{Aeq})^2}{C_{A0}.(1-X_{Aeq}).(C_{B0}-C_{A0}.X_{Aeq})} \Rightarrow$$

$$X_{Aeq} = \frac{1}{2}.\frac{-\sqrt{K_{eq}.((C_{A0}-C_{B0})^2.K_{eq}+4.C_{A0}.C_{B0})}+K_{eq}.(C_{A0}+C_{B0})}{C_{A0}.(-1+K_{eq})} \quad \text{(Eq. 7)}$$

The variables C_{A0} and C_{B0} represent the initial molar reactant concentrations [mol L^{-1}], i.e., glycerol and acetone, respectively. Hence $C_A = {}_{A0}.(1-X_A)$; $C_B = C_{B0} - (C_{A0}.X_A)$; $C_C = C_{A0}.X_A$; $C_D = C_{A0}.X_A$.

2.6 – Investigation of the Activation Energy (Ea)

The methodology for calculating the Activation Energy (E_a) was to apply a linearization tool to the Arrhenius equation [50, 51] on the values curve among the rate constants (obtained via the R2W method) (k_i) and the inverse of temperature ($1/T$), resulting in **Eq. 8**.

The kinetic reactions are run in different temperatures to calculate the Activation Energy of the catalyst . These procedures were performed via the same method as kinetic study , at temperatures between 40°C and 80°C.

$$\ln k_i = \ln k_{i_0} - \frac{Ea}{R}.\frac{1}{T} \qquad \text{(Eq. 8)}$$

where

- (k_i) = Specific rate constant for a forward or reverse reaction (mol L^{-1} min^{-1});

- (k_{i0}) = Pre-exponential factor;

- R = Universal gas constant, in this case: 8.314 J mol^{-1} K^{-1};

- T = Temperature in Kelvin (K);

- Ea = Activation Energy (kJ mol^{-1});

The result is shown in the plot $\ln(k_i)$ *versus* $1/T$.

2.7 – Catalyst Reuse

The process of reusing the catalyst has been accomplished as in the kinetic study by 1h, five consecutives reactions. At the end of each reaction, the liquid was filtered, and the zeolite was returned in the reactor for the next reaction. In fact, for this study, neither pre-treatments nor solid wash out were used. In this work, all reactions were performed in triplicate and were conducted in the same reactor. The filtered liquid portion was stored in a refrigerator for a few days prior to the analyses via a gas chromatograph flame ionization detector (GC-FID).

2.8 – Product Analyses

The products of glycerol ketalization reactions were analysed using a Shimadzu gas chromatograph with a flame ionization detector (GC-FID) via the internal standardization method. The column used was Carbowax (30 m × 0.25 mm × 0.25 µM polyethylene glycol). The internal calibration method was applied to the chromatographic patterns glycerol (99.5%) and solketal (98%) using 1,4-dioxane (99.8%) as an internal standard. The glycerol conversion calculations and solketal selectivity were performed using **Eq. 9** and **Eq. 11**:

- Glycerol Conversion (X_A):

$$X_A(\%) = \frac{N_{A0} - N_A}{N_{A0}} \cdot 100 \quad \text{(Eq. 9)}$$

N_{A0} is the initial glycerol quantity (mol), and N_A is the final quantity (mol) of the reactant.

- Selectivity (S_s):

$$Sel(\%) = \frac{A_{Product}}{A_{Products}}.100 \quad (Eq.\ 10)$$

Thus, $A_{Product}$ is associated with the desirable product, and $A_{Products}$ is the total area of desirable products and by-products in the chromatograms.

3 – RESULTS AND DISCUSSIONS

3.1 – Results of fractional factorial design

Table 1 shows the experimental design matrix (2^{4-1}), (eight experiments plus three central points) with the response to Glycerol conversion (X_A) and solketal selectivity (Ss).

Table 1 - Matrix fractional factorial design 2^{4-1} and the answers obtained for the each entry explored, using the H-BEA catalyst.

H-BEA Entry	S (rpm)	T (°C)	C (%)	RM (G:A)	X_A (%)	S_s (%)
1	400	40	1	1:2	23.80	94.30
2	400	40	5	1:4	42.24	98.17
3	400	60	1	1:4	63.21	97.65
4	400	60	5	1:2	53.13	98.07
5	700	40	1	1:4	59.34	96.16
6	700	40	5	1:2	58.99	98.18
7	700	60	1	1:2	60.36	97.71
8	700	60	5	1:4	72.62	98.30
9	550	50	3	1:3	57.57	98.00
10	550	50	3	1:3	56.51	97.76
11	550	50	3	1:3	54.76	98.45

S (Stirring); T (temperature); C (Catalyst percent); RM (molar ratio); X_A (glycerol conversion); S_s (solketal selectivity).

Table 1 shows that the best results for X_A and Ss were obtained in Entry 8, which is characterized by a temperature of 60°C, a stirring speed of 700 rpm, 5% catalyst and a molar ratio of 1:4, which are all higher than those of the other entries.

Most of the surveyed references [1, 9-18, 50, 51] and the results of this experimental design agree that, by using higher agitation speeds ($\geq$ 400 rpm), the microporous catalyst is free from any external or internal diffusional limitations in this reaction if has a molar ratio (glycerol:acetone) equal to or higher than 1:3.

Thus, it is clear, that as the molar ratio (G:A) increases, the better the conversion of glycerol. The greater the amount of acetone, the more chances for glycerol to react. Unreacted acetone can be recovered for the subsequent reactions. The amount of 5% catalyst (in relation to the mass of glycerol) is the amount usually used in industrial processes of heterogeneous catalysts. There is an increase in glycerol conversion because there is a higher amount of

available acidic sites in the catalyst (5 mass%) for the reaction compared with the 1 mass% that is used in this study. Temperature directly influences the reaction rate. Thus, the equilibrium reaction is completed in a shorter amount of time.

The fractional factorial design (2^{4-1}) results as well as a table listing their effects, X_A (glycerol conversion) and Ss (solketal selectivity), are discussed below. **Table 2** shows the effects of the variables in the conversion of glycerol (X_A).

Table 2 – Effects of each variable in the fractional factorial experiments for glycerol conversion (X_A).

Factor/H-BEA	Effect	SD	t(6)	p-value
Means	54.9	1.9	31.0	<0.05
(1) Stirring	17.1	4.0	4.2	<0.05
(2) Temperature	16.3	4.1	3.8	<0.05
(3) Catalyst	5.2	4.3	1.3	0.28
(4) Molar Ratio	10.4	4.0	2.4	<0.05

SD (Standard Deviation).

The H-BEA catalyst variables [agitation (rpm), temperature (°C) and molar ratio (G:A)] have significant and positive effects on conversion (X_A).

Then, for the H-BEA catalyst, only the catalyst variable (%) significantly affected the solketal selectivity and had a positive effect, as shown in **Table 3**.

Table 3 - Effects of each variable in the fractional factorial experiments for Solketal selectivity

(S_S).

| Factors/H-BEA	Effect	SD	t(6)	p-value
Means	97.5	0.3	350.4	<0.05
(1) Stirring	0.5	0.6	0.8	0.434
(2) Temperature	1.2	0.6	1.9	0.11
(3) Catalyst	1.7	0.6	2.7	<0.05
(4) Molar Ratio	0.5	0.6	0.8	0.47

SD (Standard Deviation).

The Solketal selectivity (S_S) occurs due to the property of selective H-BEA zeolite, which

acts as a molecular sieve.

3.2 – Kinetic Study and Determination of Kinetic Parameters

The reactions were carried out under the conditions determined by the experimental

design for 180 min, and only the temperature was varied, as shown in **Figure 1**. The conditions

were as follows: 700 rpm, a molar ratio of 1:4 (G:A), 5% catalyst relative to the mass of

glycerol, and 180 min reaction time. The results of kinetic experiments, X_A *versus* t, for various

temperatures are shown in **Figure 1**.

Figure 1 shows the experimental and R2W simulated kinetic curves.
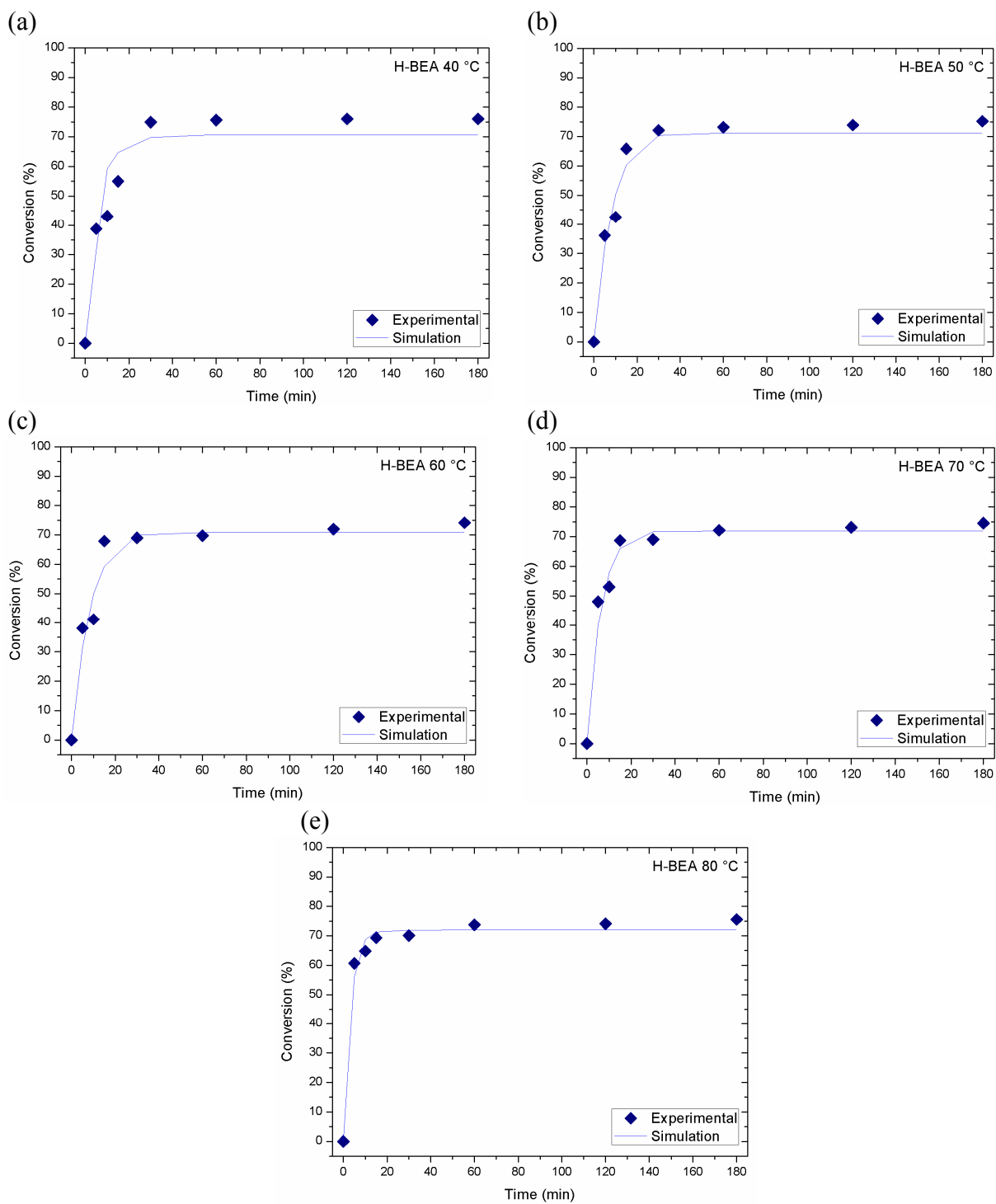
Figure 1 - Experimental and simulated via R2W kinetic curves at different temperatures. (A) 40 °C, (B) 50 °C, (C) 60 °C, (D) 70 °C, (E) 80°C.

From the simulated data shown in **Figure 1**, it was possible to determine the kinetic parameters at each temperature. Thus, the constant rates k_1 and k_{-1} were determined. Then, it was possible to calculate K_{eq} and X_{Aeq} for each temperature using the R2W simulator with an experimental data reactor feed in the ketalization reaction of glycerol with acetone using the H-BEA catalyst, as shown in **Table 4**.

Table 4 - Kinetic parameter (k_1 and k_{-1}, L mol^{-1} min^{-1}) responses calculated using R2W for the ketalization reaction of glycerol with acetone and the H-BEA catalyst.

Parameter	40 °C	50 °C	60 °C	70 °C	80 °C
k_1	0.0082	0.0085	0.0082	0.0115	0.0213
k_{-1}	0.0158	0.0159	0.0159	0.0205	0.0372
K_{eq}	0.5159	0.5366	0.5179	0.5598	0.5720
$X_{A\ EXP}$	76.01	75.17	74.16	74.52	75.54
$X_{A\ CAL}$	70.70	71.16	70.80	71.90	72.00
$X_{A\ eq\ CAL}$	70.75	71.18	70.81	71.90	72.05
Residue Q	254.22	154.77	193.22	100.50	56.58

($X_{A\ EXP}$, $X_{A\ CAL}$ and $X_{A\ eq\ CAL,}$ %; Residue Q, mol L^{-1}).

Using the reversible model, we can simplify the complex kinetics of the heterogeneous reaction through a smaller number of parameters. Thus, the parameters k_1 and k_{-1} encompass all of the kinetic terms towards the products and reactants, respectively.

The kinetics constants, which were calculated via the R2W method for evaluating the use of the H-BEA catalyst, suggest that the formation rate of Solketal is lower than the reverse (water formation) reaction rate, so that $k_1 < k_{-1}$.

From **Table 4**, it is possible to see that the k_1 and k_{-1} values increase with temperature. In all cases, the proposed kinetic model can be validated by the small difference of experimental

data conversion, $X_{A\ EXP}$ (%), in relation to the calculated conversion values, $X_{A\ CAL}$ (%). The values of Q ($0 \geq Q < 300$) show that the simulation is close to reality.

The amount of waste indicates how the observed values deviate from the simulated values [53]. This result can be attributed to the experimental error associated with the measurement. The equilibrium conversion values, $X_{A\ eq\ CAL}$, were also calculated and are close to the values of the calculated conversion at the end of the 180 min reaction. This result indicates that most of the reactions are close to equilibrium.

In the literature, there is no available information that shows a homogeneous model for the ketalization reaction of glycerol with acetone, only for the pseudo-homogeneous [51] or heterogeneous models [50, 51]. However, Esteban (2015) proposed a pseudo-homogeneous model and obtained values for $k_{-1} > k_1$ using a sulfonated resin catalyst. For the equilibrium to move towards the products, water, which is formed in the reaction system, has to be removed.

Another approach, in terms of Turnover Frequency (TOF) (the number of glycerol moles converted by moles of H-BEA acidic sites per hour), was performed at all temperatures [18], according to **Eq. 11:**

$$TOF = \frac{\left(\dfrac{N_{A0} - N_A}{N_{Cat}}\right)}{t} \qquad \text{(Eq. 11)}$$

where N_{Cat} is the number of moles of the catalyst (of acidic sites), and t is the time in hours (h) [18].

The TOF values for each temperature, at 1, 2 and 3 h, are presented in **Figure 2**.
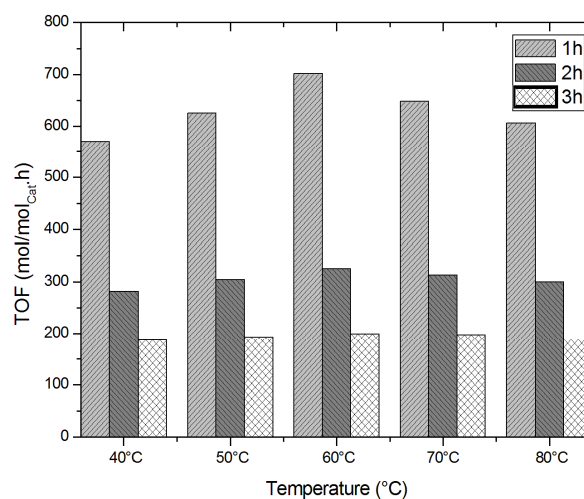
Figure 2 – Calculated TOF values at 1, 2 and 3 h and 40, 50, 60, 70 and 80°C using H-BEA as the catalyst. Conditions: 700 rpm, molar ratio of 1:4 (G:A), and 5% catalyst relative to the mass of glycerol.

The value of TOF tends to decrease with the passage of time. This observation is explained by the loss of catalytic activity or by the reaction reaching an equilibrium for reversible reactions. The best TOF value in this study, 701.12 mol/mol$_{Cat}$h, was obtained at 60°C after 1 hour of reaction. The studies by Li (2012b) reported TOF values of 54 mol/mol$_{Cat}$h for the USY zeolite and 329 mol/mol$_{Cat}$h for mesoporous silica from the TUD-1 family impregnated with Zirconium (Zr-TUD-1) after two hours of reaction. In our work, the H-BEA zeolite reached a TOF value of 325 mol/mol$_{Cat}$h.

3.3 – Investigation of Activation Energy (Ea)

Using the R2W simulator estimated kinetic parameters k_1 and k_{-1} shown in **Table 4**, it was possible to calculate the activation energy Ea for the ketalization reaction of glycerol with acetone, using the H-BEA catalyst. **Figure 3** shows the linearization of the Arrhenius equation for the forward reaction using the values found for ln (k_1) versus the inverse of temperature in Kelvin (1/T). **Figure 4** shows the linearization of the Arrhenius equation to calculate the activation energy of the reverse reaction, using the values of ln (k_{-1}) versus 1/T.
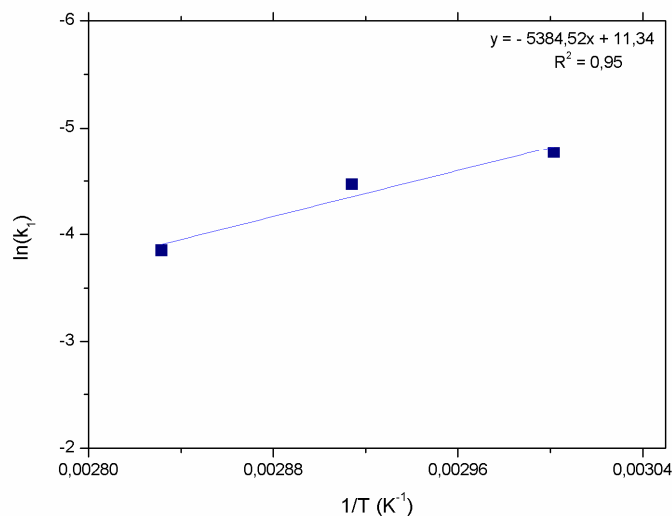
Figure 3 – Graph of ln (k_1) versus 1/T used for calculating the activation energy of the forward reaction.
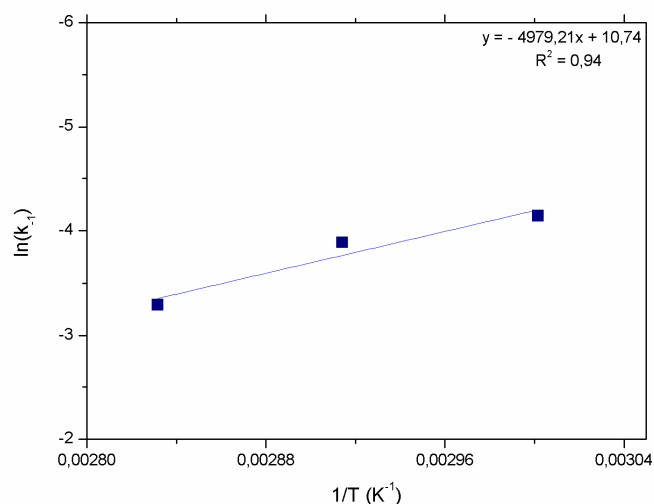
Figure 4 - Graph of ln (k_{-1}) versus 1/T used for calculating the activation energy of the reverse reaction.

To obtain a better curve fitting, the points at 40 and 50 °C were removed. **Figure 4** shows that the (-Ea/R) ratio may be obtained, whose origin is shown in **Eq. 8** in Section 2.3 of this work. The R ratio refers to the gas coefficient constant (R = 8.314 J mol^{-1} K^{-1}). Thus, in a forward reaction, (-Ea/R) = -5384.52 and Ea = 44.77 ± 1.2 kJ mol^{-1}. In the reverse reaction, (-Ea/R) = -4979.21 and Ea = 41.40 ± 1.8 kJ mol^{-1} for the 60-80°C range. In particular, an effective collision number has been calculated to be ≈ 2.4 for both the forward and reverse reactions.

Nanda (2014) determined a value of 55.6 ± 1.6 kJ mol^{-1} for the forward reaction activation energy using Amberlyst-35 resin as a catalyst [52]. Esteban (2016), using a sulfated resin as a catalyst, determined a value of 124.0 ± 12.9 kJ mol^{-1} for the activation energy of the forward reaction and 127.3 ± 12.6 kJ mol^{-1} for the activation energy of the reverse reaction [51].

It is clear that the activation energy (Ea) varies and depends on the type of catalyst and the temperature range studied. As the activation energy decreases, the speed of the reaction increases.

3.4 – Catalyst reuse research

The reuse experiments were carried out for the best fractional factorial experimental conditions, i.e., stirring at 700 rpm, a molar ratio (G:A) = 1:4, 5% zeolite mass relative to the mass of glycerol, and a 60°C reaction temperature for 1 hour. Then, after each reaction, the system was filtered, and the zeolite in the reactor was replaced for the next reaction process, up to five times. The reason why we chose to carry out the reuse tests without the need for pre-treatments (washing and calcination) of the catalyst between one reaction and another was to avoid dead time between the reactions. In industry, it is not feasible to stop production to wash and calcine the catalyst every 1h. Thus, the study was performed in a batch reactor.

Table 5 shows the results of the H-BEA catalyst reuse experiments.

Table 5 - Experimental reuse responses of the H-BEA catalyst. Conditions: 700 rpm,; molar ratio of 1:4 (G:A), 5% catalyst relative to the mass of glycerol, 60°C, and 60 min.

Time	X_A (%) ±SD	S_5 (%)±SD
1	69.74 ±0.0143	98.01 ±0.0002
2	53.52 ±0.0705	98.00 ±0.0007
3	51.49 ±0.2863	97.84 ±0.0003
4	50.91 ±0.0981	97.71 ±0.0011
5	21.61 ±0.3170	97.94 ±0.0004

SD (Standard Deviation).

According to **Table 5**, the first use of zeolite H-BEA showed the best result in catalyst reuse, i.e., approximately 70.00% glycerol conversion. From the second to the fourth reuse, activity decreases, and an average conversion of 51.97% was obtained. Thus, the catalyst showed a conversion that is similar to the one obtained in industry (52.55%) using a homogeneous catalyst (PTSA). However, from the fifth reaction, the activity decreases further, and the catalyst

converts only 21.61 ± 0.3170% of glycerol fed into the reactor. Thus, the selectivity values remain at approximately ≈ 97.99% in all experiments.

Only three publications were found regarding the research that was carried out using BEA zeolites as catalysts for the glycerol ketalization reaction with acetone [16, 55, 59].

According to the literature [57-60, 62, 63], both the Lewis acid and Brönsted sites are active during the ketalization reaction of glycerol with acetone. According to Stawicka (2016), the Brönsted acid sites were more efficient compared with Lewis acid sites or a mixture of Brönsted-Lewis acid sites [62]. For Li (2012b), Lewis acids were significantly more efficient than Brönsted acids [18].

In this work, the concentration of Brönsted acid sites (60.42 μmol of pyridine/g of H-BEA) is significantly higher than the concentration of Lewis acid sites (33.65 μmol of pyridine/g of H-BEA). There is a decrease in the amount of Brönsted acid sites with increasing temperature, while Lewis acid sites increase at higher temperatures. These results indicate that the catalyst has a higher concentration of acidic Lewis sites with a higher acidic strength than the Brönsted acid sites that present a higher concentration of weak acidic sites. Both sites were determinants for the reaction to occur. However, it is suggested that the solketal selectivity is due to the Brönsted sites, which are most effective for selectivity.

The crystallite size is the determining factor in the activity of BEA zeolite. With a smaller crystallite size, the diffusion of reactants and product molecules through zeolite channels is easier [55]. The kinetic diameters of the reactants and products in this reaction are in the range of 0.43 nm and 0.51 nm, respectively [56]. Moreover, the presence of strong acidic sites increases the catalytic activity of zeolite H-BEA. The higher the SAR of zeolite, the greater its acidic strength. Then, when the aluminium concentration decreases, glycerol conversion decreases because the

amount of weak zeolite sites increases. Nevertheless, selectivity tends to be high in both SAR situations [55].

Kowalska-Kus tested ZSM-5 zeolite in the same reaction. They suggested a reduction of the catalyst particle sizes, for lower the path of the diffusion of the reactants and products in the catalyst particle and finally, achieve higher conversion. Selectivity always remained consistent. Therefore, it can be concluded that the decrease in particle size is beneficial for the catalytic activity of the ZSM-5 zeolites for the ketalization reaction of glycerol [57].

Venkatesha (2016), using BEA zeolite without aluminium recoating, suggested that a proper combination of pore volume and acidity may be responsible for explaining the selectivity of 100% solketal. The increased number of acidic sites may be responsible for causing the hydrolysis products to favour the reverse reaction that returns glycerol and acetone to the reaction medium. The reduction in the amount of aluminium catalyst acidity decreases, and consequently reduces the hydrolysis products. The aluminium removal causes increased hydrophobicity in the zeolitic channels by preventing hydrolysis of the product [55, 58, 59].

In this work, we used an H-BEA zeolite type with a crystallite size equal to 13 nm (SAR $\approx$ 19) and a 10 μm average particle size.

After the catalyst reuse study, the H-BEA zeolite lost a significant amount of area and micropore area. The volume of the mesoporous portion (BJH) and the size of mesopores (BJH) also significantly decreased. The decrease in these values, as shown in **Table 6**, added to the loss of crystallinity of H-BEA, as shown by the XRD patterns in **Figure 5**. Combined with the abovementioned theory, the blocking of active sites by the molecules of water that are formed during the reaction may explain the loss of the H-BEA catalyst activity. The mesoporous portion in microporous materials is obtained via industrial synthesis (large scale). The clustering of these

particles results in mesoporous spaces between them. The mesoporous portion in microporous

materials not ocur with laboratorial synthesis (small scale).

Table 6 - Textural characteristics of the H-BEA catalyst before and after the reuse experiments.

Result	H-BEA	Post reuse
Area BET $[m^2\ g^{-1}]$	536	513
Area MICROPORES $[m^2\ g^{-1}]$	338	313
Area EXTERNAL $[m^2\ g^{-1}]$	199	200
Volume TOTAL $[cm^3\ g^{-1}]$	0.57	0.52
Volume MICROPORES $[cm^3\ g^{-1}]$	0.16	0.14
Volume BJH/DES $[cm^3\ g^{-1}]$	0.52	0.39
Pore Size BET $[nm]$	4.10	4.00
Pore Size BJH/DES $[nm]$	13.70	10.60
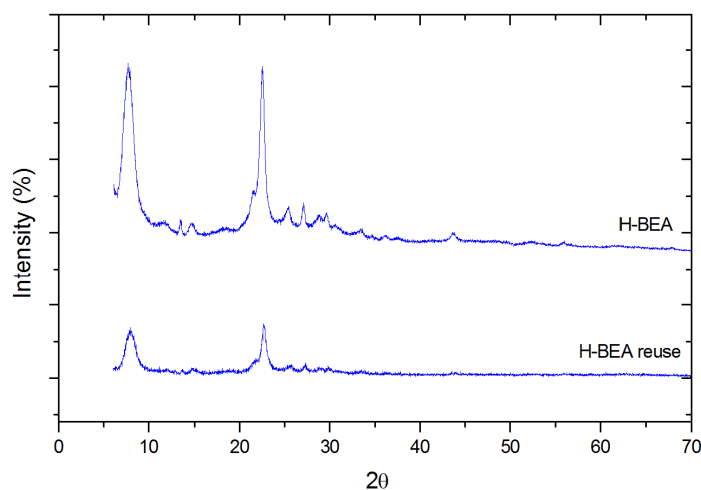
Figure 5 – X-ray diffraction pattern of the H-BEA catalyst before and after reuse experiments.

It is very likely that some of the water that is formed during the reaction and/or reactant impurities, such as sodium residue in glycerol, caused destabilization of the H-BEA zeolite structure. Thus, this phenomenon altered its crystallinity and decreased its activity, resulting in a possible deactivation of acidic sites as well as pore reduction. However, this issue should be further explored in other studies.

Even if acidic catalysts have high activity, they can be deactivated by having their active sites blocked by water molecules formed during the reaction [16]. The higher hydrophobicity of the smallest catalyst is due to the number of acidic sites. However, the hydrophobic groups act at the glycerol acetone interface and reduce the interference of water molecules on the surface of the catalyst [60]. The deactivation of zeolites is often due to the formation of by-products within the pores or on the outer surface of crystallites, which block access of the reactant to the acidic site [65]. To avoid deactivation of the catalyst, an alternative is to increase the reactor temperature [66].

Currently, our research group is conducting a new study. The use of reactor recycling has shown good glycerol conversion results for the reuse of the H-BEA catalyst and has shown high catalytic activity for up to 8 treatments without pre-treatment between reactions. However, the study is very recent and requires additional work before it is published.

4 – CONCLUSIONS

From the reaction kinetic reversible model it was possible to represent the experimental data of glycerol ketalization for the production of Solketal. The inverse routine applied (R2W) led to a good fit between the experimental data and the simulation results that validates the utilization of such a kinetic model for each temperature reactions. The veracity of the kinetic constants is verified through the comparison between the experimental and calculated conversion

values at the equilibrium obtained from the equilibrium constants and confirmed by equilibrium

conversion and Q value. A Statistical treatment of the experimental data can be used to improve

the accuracy in the estimation of the kinetic constants. The activation energy Ea value was

calculated. The use of H-BEA zeolite as a catalyst during the production of Solketal was been

shown to be efficient and achieve high conversion and selectivity under mild conditions. Thus, it

is feasible to use the H-BEA catalyst in industrial processes for the production of Solketal.

Furthermore, it can be used for four consecutive times.

AUTHOR INFORMATION

Corresponding Author:

*Vinicius Rossa (DSc. Student and Researcher): **vinnyrossa@gmail.com**

Author Contributions:

   The authors of this work include Vinicius Rossa (main author, Doctoral Student and

Researcher); Yolanda SP Pessanha (Master); Gisel Ch. Díaz (Post-Doctoral Fellow); and Sibele

B. C. Pergher, Leôncio D. T. Câmara e Donato and A. G. Aranda (Post-Doctoral Professors at

UFRN, UERJ and UFRJ, respectively). The manuscript was written comprising contributions of

all authors. All authors have approved the final version of the manuscript.

ABBREVIATIONS

PTSA: p-toluenesulfonic acid;

BEA: β-Zeolite;

BEA-NH_4^+: β-Zeolite in ammonium form;

H-BEA: acidic β-Zeolite;

BS: Brönsted Acid Sites;

LS: Lewis Acid Sites;

R2W: Random Restricted Window (Inverse Stochastic Routine);

Ea: activation energy (kJ mol^{-1});

SAR: Silica alumina ratio;

X_A: Glycerol conversion;

S_S: Solketal Selectivity;

k_1: forward reaction kinetic constant, L mol^{-1} min^{-1};

k_{-1}: reverse reaction kinetic constant, L mol^{-1} min^{-1};

T: temperature (°C-Celsius or K-Kelvin);

R: universal gas constant (8.314 J mol^{-1} K^{-1});

$X_{A\ eq}$: glycerol conversion in equilibrium;

K_{eq}: equilibrium constant;

Q: square residue;

TOF: Turnover frequency;

SD: standard deviation.

1
2
3
4
5
6
7
8
9
10
11
12
13
14
15
16
17
18
19
20
21
22
23
24
25
26
27
28
29
30
31
32
33
34
35
36
37
38
39
40
41
42
43
44
45
46
47
48
49
50
51
52
53
54
55
56
57
58
59
60

REFERENCES

(1) Mota, C. J. A.; Silva, C. X. X. ; Gonçalves, V. L. C., Gliceroquímica: novos produtos e processos a partir da glicerina de produção de biodiesel. Quim. Nova, 2009, 32, 3, 639-648.

(2) Adhikari, S., Fernando, S., Haryanto, A., Production of hydrogen by steam reforming of glycerin over alumina-supported metal catalysts, Catal. Today, 2007, 129, 355-364.

(3) Sánchez, E.A., D'Angelo, M.A., Comelli, R.A., Hydrogen production from glycerol on Ni/Al$_2$O$_4$ catalyst, Int. J. Hydrogen Energy, 2010, 35, 5902-5907.

(4) Kim, B. C.; Lee, J.; Um, W.; Kim, J.; Joo, J.; Lee, J. H.; Kwak, J. H.; Kim, J. H.; Kirschhock, C. E. A.; Sultana, A.; Godard, E.; Martens, J. A., Adsorption Chemistry of Sulfur Dioxide in Hydrated Na–Y Zeolite, Angew. Chem. Int. Ed., 2004, 43, 3722-3724.

(5) Agirre,I.; Garcia, I.; Requies, J.; Barrio, V. L.; GüemeZ, M.B.; Cambra, J.F.; Arias, P.L., Glycerol acetals, kinetic study of the reaction between glycerol and formaldehyde, Biomass Bioenergy, 2011, 35, 3636-3642.

(6) Serafim, H.; Fonseca, I.M.; Ramos, A.M.; Vital, J.; Castanheiro, J.E., Valorization of glycerol into fuel additives over zeolites as catalysts, Chem. Eng. J., 2011, 178, 291– 296.

(7) Silva, P. H. R.; Gonçalves, V. L.C.; Mota, C. J.A., Glycerol acetals as anti-freezing additives for biodiesel, Bioresour. Technol., 2010, 101, 6225–6229.

(8) Deutsch, J.; Martin, A.; Lieske, H.; Investigations on heterogeneously catalysed condensations of glycerol to cyclic acetals, J. Catal. , 2007, 245, 428.

(9) Royon, D.; Locatelli, S.; Gonzo, E.E., Ketalization of glycerol to solketal in supercritical acetone, J. Supercrit. Fluids, 2011, 58, 88-92.

(10) Reddy, P. S.; Sudarsanam, P.; Mallesham, B.; Raju, G.; Reddy, B. M., Acetalisation of glycerol with acetone over zirconia and promoted zirconia catalysts under mild reaction conditions, J. Ind. Eng. Chem., 2011, 17, 377-381.

(11) Gelas, J., Acétals cycliques derives de la glycérine. Bull. Soc. Chim. Fr., 1970, 6, 2341-2353.

(12) Khayoon, M.S.; Hameed, B.H., Solventless acetalization of glycerol with acetone to fuel oxygenates over Ni–Zr supported on mesoporous activated carbon catalyst, Appl. Catal., A, 2013, 464-465, 191-199.

(13) Suriyaprapadilok, N.; Kitiyanan, B., Synthesis of Solketal from Glycerol and Its Reaction with Benzyl Alcohol, Energy Procedia, 2011, 9, 63-69.

(14) Menezes, F. D. L.; Guimaraes, M. D. O.; Silva, M. J. D., Highly Selective SnCl$_2$-Catalyzed Solketal Synthesis at RoomTemperature, Ind. Eng. Chem. Res. , 2013, 52, 16709−16713.

(15) Ferreira, P.; Fonseca, I.M.; Ramos, A.M.; Vital, J.; Castanheiro, J.E, Valorisation of glycerol by condensation with acetone over silica-included heteropolyacids, Appl. Catal., B, 2010, 98, 94–99.

(16) Silva, C. X. A. D.; Mota, C. J. A., The influence of impurities on the acid-catalyzed reaction of glycerol with acetone, Biomassa Bioenergy, 2011, 35, 3547-3551.

(17) Li, F.; Xue, F.; Chen, B.; Huang, Z.; Yuan, Y.; Yuan, G., Direct catalytic conversion of glycerol to liquid-fuel classes over Ir–Re supported on W-doped mesostructured sílica, Appl. Catal., A, 2012a, 449, 163-171.

(18) Li, L., Korányi, T. I.; Sels , B. F.; Pescarmona, P. P., Highly-efficient conversion of glycerol to solketal over heterogeneous Lewis acid catalysts, Green Chem. , 2012b, 14, 1611.

(19) Li, J.; Wang, T., Chemical equilibrium of glycerol carbonate synthesis from glycerol, J. Chem. Thermodyn., 2011, 43, 731–736.

(20) Zheng, Y.; Chen, X.; Shen, Y., Commodity chemicals derived from glycerol, an importantebiorefinery feedstock, Chem. Rev., 2008, 108, 12, 5253-5277.

(21) Fujita, S.; YAmanishi, Y.; Arai, M., Synthesis of glycerol carbonate from glycerol and urea using zinc-containing solid catalysts: A homogeneous reaction, J. Catal., 2013, 297, 137–141.

(22) Aresta, M.; Dibenedetto, A.; Nocito, F.; Ferragina, C., Valorization of bio-glycerol: New catalytic materials for the synthesis of glycerol carbonate via glycerolysis of urea, J. Catal., 2009, 268, 106–114.

(23) Climent, M. J.; Corma, A.; Frutos, P. D.; Iborra, S.; Noy, M.; VElty, A.; Concepción, P., Chemicals from biomass: Synthesis of glycerol carbonate by transesterification and carbonylation with urea with hydrotalcite catalysts. The role of acid–base pairs, J. Catal., 2010, 269, 140–149.

(24) Wang, L.; Ma, Y.; Wang, Y.; Liu, S.; Deng, Y., Efficient synthesis of glycerol carbonate from glycerol and urea with lanthanum oxide as a solid base catalyst, Catal. Commun., 2011, 12, 1458–1462.

(25) Jagadeeswaraiah, K.; Kumar, C. R.; Prasad, P. S. S.; Loridant, S.; Lingaiah, N., Synthesis of glycerol carbonate from glycerol and urea overtin-tungsten mixed oxide catalysts, Appl. Catal., A, 2014., 469, 165– 172.

(26) Turney, T. W.; Patti, A.; Gates, W.; Shaheen, U.; Kulasegaram, S., Formation of glycerol carbonate from glycerol and urea catalysed by metal monoglycerolates, Green Chem. , 2013, 15, 1925-931.

(27) George, J.; Patel, Y.; Pillai, S. M.; Munshi, P., Chemical equilibrium of glycerol carbonate synthesis from glycerol, J. Mol. Catal. A: Chem., 2009, 304, 1-7.

(28) Alvarez, M.G.; Frey, A.M.; Bitter, J.H.; segarra, A.M.; Jong, K.P.; Medina, F., On the role of the activation procedure of supported hydrotalcites for basecatalyzed reactions: Glycerol to glycerol carbonate and self-condensation of acetone, Appl. Catal., B, 2013, 134-135, 231– 237.

(29) Ramaya, S.; Brittain, A.; De Almeida, C.; Mok, W.; Antal, M. J.; Acid-catalysed dehydration of alcohols in supercritical water, Fuel, 1987, 66, 1364.

 (30) Klepácová, K.; Mravec, D.; Hajekova, E.; Bajus, M.; Etherification of Glycerol, Pet. Coal, 45, 54, 2003.

(31) March, J.; Advanced Organic Chemistry. Reactions, Mechanisms and Structure, Wiley: New York, 4th ed., p. 386, 1992.

(32) Mota, C. J. A.; Gonçalves, V. L. C., Br PI 0700063-4, 2007.

(33) Delagado, J.; Es Pat. 2201894, 2002.

(34) Garcia, E.; Laca, M.; Pérez, E.; Garrido, A.; Peinado, J.; New Class of Acetal Derived from Glycerin as a Biodiesel Fuel Component, Energy Fuels, 22, 4274, 2008.

(35) Melero, J. A.; Van Grieken, R.; Morales, G.; Paniagua, M.; Acidic Mesoporous Silica for the Acetylation of Glycerol: Synthesis of Bioadditives to Petrol Fuel, Energy Fuels, 2007, 21, 1782.

(36) Liao, X.; Zhu, Y.; .Wang, S.G.; Li, Y. Producing triacetylglycerol with glycerol by two steps: esterification and acetylation, Fuel Process. Technol., 2009, 90, 988–993.

(37) Chaminand, J.; Djakovitch, L.; Gallezot, P.; Marion, P.; Pinel, C.; Rosinerb, C.; Glycerol hydrogenolysis on heterogeneous catalysts, Green Chem., 2004, 6, 359.

(38) Maris, E.; Davis, R., Hydrogenolysis of Glycerol over Carbonsupported Ru and Pt Catalysts, J. Catal., 2007, 249, 328.

(39) Allhanash, A.; Koszhevnikova, E.; Kozhevnikov, I. Hydrogenolysis of Glycerol to Propanediol over Ru:Polyoxymetalate Bifunctional Catalyst, Catal. Lett., 2008., 120, 307.

(40) Yuan, Z.; Wang, J.; Wang, L.; Xia, S.; Chen, P.; Z. Hou; Zheng, X., Hydrogenolysis of glycerol over homogenously dispersed copper on solid base catalysts, Appl. Catal., B, 101, 431-440.

(41) Dauenhauer, P.; Salge, J.; Schmidt, L., Renewable Hydrogen by Autothermal Steam Reforming of Volatile Carbohydrates, J. Catal., 2006, 244, 238.

(42) Akiyama, M.; Sato, S.; Takahashi, R.; Inui K.; Yokota M., Dehydration–hydrogenation of glycerol into 1,2-propanediol at ambient hydrogen pressure, Appl. Catal., A, 2009, 371, 60–66.

(43) Beatriz, A.; Araújo, Y. J. K.; Lima, D. P., Glicerol: um breve histórico e aplicação em sínteses estereosseletivas, Quim. Nova, 2011, 34, 2, 306-319.

(44) Bauer, R.; Hekmat, D.; Biotechnol. Prog., 2006, 22, 278.

(45) Gates, B. C.; Catalytic Chemistry, Wiley: New York, cap. 5, 1992.

(46) Clark, J. H.; Macquarrie, D. J., Handb. Green Chem. Technol., Blackwell Science Ltd.: Oxford, 2002.

(47) Hagen, J. Industrial Catalysis: A Practical Approach, 2nd Ed.; Wiley-VCH Verlag GmbH & Co. KGaA: Weinheim, Capítulo 1, 1-13, 2006.

(48) Moreno, E. L.; Rajagopal, K., Desafios da acidez na catálise do estado sólido, Quim. Nova, 2009, 32, 2, 538-542.

(49) Câmara, L. D. T.; Cerqueira, H. S.; Aranda, D. A. G.; Rajagopal, K., Application of a three-dimensional network model to the coke formation in FAU, MFI and BEA zeolites, Catal. Today, 2004, 98, 309.

(50) Nanda, M. R.; Yuan, Z.; Qin, W.; Ghaziaskar, H. S.; Poirier, M.; Xu, C. C. Thermodynamic and kinetic studies of a catalytic process to convert glycerol into solketal as an oxygenated fuel additive, Fuel, 2014, 117, 470–477.

(51) Esteban, J.; Ladero, M.; Garcia-Ochoa, F., Kinetic modelling of the solventless synthesis of solketal with a sulphonic ion exchange resin, Chem. Eng. J., 2015, 269, 194–202.

(52) Câmara, L. D. T.; Silva Neto, A. J. Inverse Stochastic Characterization of Adsorption Systems by a Random Restricted Window (R2W) Method., Eng. Opt, Rio de Janeiro, 2008.

(53) Câmara, L. D. T.; Aranda, D. A. G.,Reaction Kinetic Study of Biodiesel Production from Fatty Acids Esterification with Ethanol, Ind. Eng. Chem. Res., 2010, 50, 2544-2547.

(54) Rodrigues, M. A.; Iemma, A. F., Planejamento de Experimentos e Otimização de Processos: uma estratégia sequencial de planejameto, editora Casa do Pão, ed. 1, UNICAMP, Campinas/SP, 2005.

(55) Manjunathan, P.; Maradur, S. P.; Halgeri, A.B.; Shanbhag, G. V., Room temperature synthesis of solketal from acetalization of glycerol with acetone: Effect of crystallite size and the role of acidity of beta zeolite, J. Mol. Catal. A: Chem., 2015, 396, 47–54.

(56) Frisch, M. J.; Gaussian 03, Revision B.01. Gaussian, Inc., Pittsburgh, 2003.

(57) Kowalska-Kus, J.; Held, A.; Nowinska, K.; Enhancement of the catalytic activity of H-ZSM-5 zeolites for glycerol acetalization by mechanical grinding, React. Kinet., Mech. Catal., 2016, 117, 341–352.

(58) Gadamsetti, S.; Rajan, N. P.; Rao, G. S.; Chary, K. V. R., Acetalization of glycerol with acetone to bio fuel additives oversupported molybdenum phosphate catalysts, J. Mol. Catal. A: Chem., 2015, 410, 49–57.

(59) Venkatesha, N. J.; Bhat, Y. S.; Jai Prakash, B. S., Dealuminated BEA zeolite for selective synthesis of five-membered cyclic acetal from glycerol under ambient conditions, RSC Adv., 2016, 6, 18824-18833.

(60) Sandesh, S.; Halgeri, A.B.; Shanbhag, G. V., Utilization of renewable resources: Condensation of glycerol with acetone at room temperature catalyzed by organic–inorganic hybrid catalyst, J. Mol. Catal. A: Chem., 2015, 401, 73–80.

(61) Emmeis, C. A., Determination of Integrated Molar Extinction Coefficients for Infrared Absorption Bands of Pyridine Adsorbed on Solid Acid Catalysts, J. Catal., 1993, 141, 347-354.

(62) Stawicka, K.; Díaz-Álvarez, A. E.; Calvino-Casilda, V.; Trejda, M.; Bañares, M. A.; Ziolek, M., The Role of Brønsted and Lewis Acid Sites in Acetalization of Glycerol over Modified Mesoporous Cellular Foams, J. Phys. Chem. C, 2016, 120, 16699−16711.

(63) Nanda, M. R.; Zhang, Y.; Yuan, Z.; Qin, W.; Ghaziaskar, H. S.; Xu, C C., Catalytic conversion of glycerol for sustainable production of solketal as a fuel additive: A review, Renewable Sustainable Energy Rev., 2016, 56, 1022–1031.

(64) Sie, S.T., Consequences of catalyst deactivation for process design and operation, Appl. Catal., A, 2001, 212, 129-151.

(65) Rohan, D.; Canaff, C.; Magnoux, P.; Guisnet, M., Origin of the deactivation of HBEA zeolites during the acylation of phenol with phenylacetate, J. Mol. Catal. A: Chem., 1998, 129, 69-78.

(66) Forzatti, P.; Lietti, L., Catalyst deactivation, Catal. Today, 1999, 52, 165-181.

1
2
3   TOC:
4
5
6
7
8
9
10
11
12
13
14
15
16
17
18
19
20
21
22
23
24
25
26
27
28
29
30
31
32
33
34
35
36
37
38
39
40
41
42
43
44
45
46
47
48
49
50
51
52
53
54
55
56
57
58
59
60